

A FAST NUMERICAL APPROACH TO REDUCE VOID FORMATION IN LIQUID COMPOSITE MOLDING

Edu Ruiz^{(a)(*)}, V. Achim^(a), J. Bréard^(b), S. Chatel^(c) and F. Trochu^(a)

(a) *Chaire sur les Composites à Haute Performance (CCHP), Centre de Recherches En Plasturgie Et Composites (CREPEC), Département de génie mécanique,*

École Polytechnique, Montréal (Québec) HC 3A7 <http://cchp.meca.polymtl.ca>

(b) *Laboratoire de Mécanique, Physique et Géosciences, Université du Havre, Quai Frissard, BP 540, 76058 Le Havre Cedex, France*

(c) *European Aeronautic Defense and Space Company, Corporate Research Centre (EADS CCR), 12 rue Pasteur BP 7692152 Suresnes Cedex, France*

(*)e-mail: edu.ruiz@polymtl.ca

ABSTRACT: Liquid Composite Molding (LCM) regroups a number of well known manufacturing techniques of fiber-reinforced polymer composites based on resin injection through fibrous reinforcements. LCM processes such as RTM (Resin Transfer Molding) have been increasingly used to manufacture parts for a wide range of industrial applications and were shown to be cost-effective in the low to medium range of volume production. To improve the performance of these processes, more scientific knowledge of the impregnation phenomena is required. It has been recently observed that the resin velocity during impregnation of the fibrous preform is a key factor that governs the formation of macro/micro voids trapped between or inside the fiber tows. An inverse relationship of the volume of macro/micro voids with the fluid velocity indicates the existence of an optimum velocity that minimizes the void formation during mold filling. In this work, a new numerical simulation and process optimization procedure is proposed to minimize void formation during the filling stage in LCM. The approach consists of calculating the flow rate to be injected at each time step in order to guarantee an optimum impregnation velocity at the flow front that minimizes the formation of macro/micro voids. Experimental injections were conducted to validate the proposed approach. A test case was carried out on a composite part to highlight the advantages of the proposed optimization. This numerical tool brings an added value to standard LCM simulations and opens up the scope of a whole range of new applications of process optimization.

INTRODUCTION

During the past years, polymer composite applications have gained ground for technological, economical and environmental reasons. The aerospace, marine and automotive industries have pioneered the use of high performance composites in numerous structural and semi-structural applications. Nowadays, a wide number of applications have appeared in different fields such as biomedicine, petroleum plants, bridges, etc. Liquid Composite Molding (LCM) regroups a number of techniques to manufacture fiber-reinforced polymer composites. LCM processes such as Resin Transfer Molding (RTM) have been increasingly used to manufacture parts for a wide range of industrial applications demonstrating the cost effectiveness of this technology in the low to medium range of volume production. In RTM manufacturing, during the injection stage, a liquid resin impregnates the fibers before it cures and solidifies. If the fibrous reinforcement is not fully impregnated, voids are created resulting in a decrease of

mechanical properties and surface quality of the part. To improve process performance, void formation during resin impregnation must be reduced. The fibers typically used in LCM are described as a dual-scale porous medium [1]. As shown in Fig. 1 for a unidirectional glass fabric, porosities can be observed at two identifiable scales. Porosities at the macroscopic scale are defined as the free spaces between fabric tows (see Fig. 1(a)), while the microscopic scale represents the free spaces between tows (see Fig. 1(b)). This double scale porous medium leads to a two-level impregnation mechanism (i.e., filling of the micro and macro-pores). Researchers have experimentally studied the infiltration phenomena and concluded that the resin velocity influences the formation and location of the voids in the part [1, 2]. During impregnation of a double-scale porous medium, the forces that induce the motion of the fluid are of two different nature: the viscous and the capillary forces. Bréard et al. [1] carried out a microscopic study of the porosity and void content of RTM composite specimens manufactured at different injection flow rates. It was found that for low resin velocities, the capillary forces become dominant inducing the fluid flow to travel through the fabric tows, where the porosity is smaller and the total surface tension higher. As shown in Fig. 2(a), in the case of capillary dominant flows, macro-voids can be trapped in the open spaces between fiber tows. In the opposite case, for high resin velocities, the viscous forces are predominant forcing the fluid flow to travel through the open spaces between tows (see Fig. 2(b)). As depicted in the microscopic image on Fig. 2(b), in case of viscous dominant flow, microscopic voids appear inside the fiber tows due to the difference between the viscous resistance in the tows and in the open channels. In the past, researchers have published several experimental investigations on the formation of micro and macro-voids [1-4]. Some analyses were also performed to identify and describe the mechanisms of void formation [5-6]. In practice, the injection flow rate should be optimized and controlled to minimize void formation. Numerical simulation is a useful tool of virtual prototyping in composite manufacturing. Computer analyses are addressed to model, predict and control the events that occur during the fabrication of LCM parts, although no much information is given about the impregnation of the fibers. In this work, a practical numerical methodology is presented to calculate the optimum injection flow rate that minimizes void formation and improves RTM processing. The proposed numerical approach results in a fast calculation of the optimal transient injection rate to open/close the injection gates and vents even in the non-isothermal case.

OPTIMAL IMPREGNATION VELOCITY

Various researches [7-9] have demonstrated that the percentage of macro/micro-voids formation is a near logarithmic function of the fluid flow velocity (v). As shown in Fig. 3, the volume of macro and micro void formation can be estimated as an inverse logarithmic function of the impregnation velocity. In this work, void formation was measured for three kinds of reinforcements: a monofilament mat Unifilo 101 from Vetrotex, a bi-directional glass fabric NCS 82620 and a woven fabric consisting of single end glass rovings Rovcloth 2454 from Fiber Glass Industries. For each reinforcement rectangular composite plates of 35 x 25 cm and 3 mm thick were impregnated with an epoxy resin. For each composite plate manufactured, the resin injection flow rate was varied between 6 and 18 ml/sec and the void content measured by comparison with the composite density (following the norms ASTM D792-00 and ASTM D3171-99). As depicted in Fig. 4 for the Unifilo 101, a nearly constant void formation was observed along the length of the composite plates. The figure also highlights the influence of the injection flow rate (or injection velocity) on the formation of voids. This experimental analysis demonstrates the existence of an optimal injection velocity that minimizes the void formation in the fibrous reinforcement [2, 7]. Instead of relating the

fluid velocity to the percentage of voids trapped, researchers [2-4, 7-9] have used an dimensionless parameter called the *capillary number* (Ca). This dimensionless number represents the relative effect of viscous forces and surface tension acting across an interface between a liquid and a gas. It takes the following form:

$$Ca = \frac{\mu v}{\gamma} \quad (1)$$

where μ the viscosity of the fluid, γ the surface tension at the interface air/resin and v is the fluid velocity. Patel et al. [2] measured the voids trapped for a large number of fluids and flow velocities. When void fractions are plotted against Ca , the experimental curves merged into a master characteristic curve. Void formation measured as a function of fluid velocity (as shown in Fig. 4) can then be transformed into a function of Ca . Using the surface tension characterized by Patel et al. [2] for an epoxy resin $\gamma = 35$ mN/m and a resin viscosity of $\mu = 0,1$ Pa.s, the measured void contents were compared for the three reinforcements as a function of Ca (see Fig. 5). It can be observed that minimum void formation is obtained for a Ca of $3,8 \times 10^{-2}$ for the Unifilo 101, while the FGI and NCS fabrics appear to have a minimum number of voids at lower Ca (not allowed by the injection system used in this work).

OPTIMIZATION OF THE INJECTION FLOW RATE

As detailed in [10], once an optimal capillary number is identified for a combination of resin and fibers, the optimal impregnation velocity (v_{imp}^{opt}) can be calculated as follows:

$$v_{imp}^{opt} = \frac{Ca_{opt} \gamma}{\mu} \quad (2)$$

Darcy's law is widely used to model the fluid flow through porous media. It establishes the relationship between the fluid velocity and pressure gradient ∇P :

$$\vec{v}_{front} = -\frac{[K]}{\mu\phi} \nabla P \quad (3)$$

where \vec{v}_{front} is the fluid macroscopic velocity at the flow front, $[K]$ is the permeability tensor of the porous medium, μ is the resin viscosity and ϕ is the total porosity of the dual-scale porous medium. Assuming that the micro/macro voids appear in the partially saturated regions near the flow front, the injection flow rate can be optimized by setting the front velocity equal to the optimal impregnation velocity:

$$\|\vec{v}_{front}^{opt}\| = v_{imp}^{opt} \quad (4)$$

Neglecting the mold deformation, the global mass balance of the fluid indicates that the flow rate across the fluid flow front Q_{front} is equal to the flow rate Q_{inj} injected at the inlet gate:

$$Q_{front} = Q_{inj} \quad (5)$$

In a finite element control volume simulation (FE-CV), for a given time step (i.e., a step during part filling) the flow rate at the flow front Q_{front} is calculated by the flow front velocity $\|\vec{v}_{front}\|$ passing through the flow front area A_{front} :

$$Q_{front} = A_{front} \|\vec{v}_{front}\| \quad (6)$$

The optimal flow rate at the flow front Q_{front}^{opt} (i.e., the flow rate that minimizes void formation), can be calculated by considering the flow front area and the optimal impregnation velocity as follows:

$$Q_{front}^{opt} = A_{front} \cdot \|\vec{v}_{front}^{opt}\| = A_{front} \cdot v_{imp}^{opt} \quad (7)$$

If an optimal impregnation velocity is desired at the flow front, the flow rate Q_{front} may be corrected in the following way:

$$\frac{Q_{front}}{Q_{front}^{opt}} = \frac{\|\vec{v}_{front}\|}{v_{imp}^{opt}} \quad (8)$$

To correct Q_{front} , the injection flow rate must be modified. To do so, an initial injection flow rate is corrected with the ratio between the calculated flow front velocity and the optimal impregnation velocity as expressed in equation (8). Regrouping equations (5) and (7), for closed loop iteration in k , the corrected injection flow rate that minimizes the formation of macro/micro voids is:

$$Q_{inj}|_{k+1} = \left(\frac{v_{imp}^{opt} Q_{inj}}{\langle \|\vec{v}_{front}\| \rangle} \right)_k \quad (9)$$

where $\langle \|\vec{v}_{front}\| \rangle$ is the averaged flow front velocity for all the elements located on the flow front calculated in the following way:

$$\langle \|\vec{v}_{front}\| \rangle = \sum_{i=1}^n \|\vec{v}_i / \phi_i\| / n \quad (10)$$

Combining equations (1), (2) and (4), equation (10) can now be expressed as a function of the optimal capillary number as follows:

$$Q_{inj}|_{k+1} = \left(\frac{Ca_{opt} Q_{inj}}{\langle \|Ca_i\|_{i=1,n} \rangle} \right)_k \quad (11)$$

The proposed optimization is limited to flows where velocity variations at the flow front are not too high. This is the case for preforms with very different permeabilities or parts of complex geometries where the flow is separated to travel around inserts. Note that even on these cases, the proposed methodology will reduce the formation of macro/micro voids compared to a non-controlled injection. Open channels (such as edge effects) should not be considered in this calculation because macro/micro voids are not trapped in these free spaces.

NUMERICAL IMPLEMENTATION

The numerical implementation of the optimization algorithm is based on a finite element approximation [11] of Darcy equation combined with an iterative procedure to correct the injection flow rate as proposed by equation (11). The algorithm starts with a standard filling simulation with the optimal impregnation velocity v_{imp}^{opt} imposed at the injection gate. The averaged capillary number $\langle \|Ca_{opt}\|_{i=1,n} \rangle$ is then extracted from the finite elements at the flow front. This capillary number is then used in equation (11) to rescale the injection flow rate. For each time step, a closed loop iteration is performed until the averaged capillary number in the vicinity of the flow front approaches the optimal value Ca_{opt} . The resulting injection flow rate is then used as a new boundary condition to advance the flow front to a new transient position defined by the filling algorithm. Finally, a new time step is computed, and the iterative process repeated until the mold is totally filled.

APPLICATION EXAMPLE

To illustrate the capabilities of the proposed optimization procedure, an application example was performed for an automotive part. The isothermal filling of a car hood (see Fig. 6) was simulated at constant injection pressure, constant injection flow rate and with the optimized injection flow rate from equation (11). Fig. 7 shows a comparison of the void formation calculated for the three injection strategies simulated.

The injection performed at constant pressure shows a high formation of voids (around 4%) at the middle of the radial geometry resulted from the central injection (see Fig. 7(a)). Similar results were obtained for an injection at constant flow rate because of the variations of the flow front velocity during filling of the car hood (see Fig. 7(b)). To optimize filling, the injection flow rate was adjusted in order to keep the capillary number at the optimum value. The final void distribution of Fig. 7(c) shows that the void formation decreased to nearly zero when the optimized injection is applied. Therefore the optimization strategy allowed reducing the total void content to a minimum, which will result in better mechanical properties for the final part.

CONCLUSIONS

This study concerns the optimization of the injection flow rate to minimize the void formation in composite parts manufactured by Resin Transfer Molding. The quality and mechanical performance of composite parts is strongly dependent on the percent of macro/micro voids. In this work, an optimization methodology was presented to reduce the percent of macro/micro voids formed during RTM manufacturing. The optimization is based on the optimal capillary

number at the fluid flow front position. To demonstrate the capabilities of the proposed algorithm, a test case on an automotive part was presented. The optimized injection (calculated with the proposed algorithm) was compared with an injection at controlled resin pot pressure. The optimization showed a minimization of the void formation for similar filling times. Finally, the injection optimization proposed in this work is shown to be a useful tool to minimize the percentage of voids formed within the fibrous reinforcement and increase the performance of composite parts by injection molding.

ACKNOWLEDGEMENTS

The authors are grateful to the National Science and Engineering Research Council of Canada (NSERC) and Fonds Québécois de Recherche sur la Nature et la Technologie (FQRNT) for their financial support. The authors would also like to thank CREPEC (Centre de recherche en plasturgie et composites) and ESI-Group for supporting this work.

REFERENCES

1. J. Breard, Y. Henzel, F. Trochu, R. Gauvin, "Analysis of dynamic flows through porous media. Part I: Comparison between saturated and unsaturated flows in fibrous reinforcements", *Polymer Composites*, Vol. 24, no. 3, 2003, pp. 391.
2. N. Patel, L.J. Lee, "Effects of fiber mat architecture on void formation and removal in liquid composite molding", *Polymer Composites*, Vol. 16, no. 5, 1995, pp. 386.
3. G.W. Lee, K.J. Lee, "Mechanism of void formation in composite processing with woven fabrics", *Polymer & Polymer Composites*, Vol. 11, no. 7, 2003, pp. 563.
4. A.D. Mahale, R.K. Prud'Homme, L. Rebenfield, "Characterization of voids formed during liquid impregnation of non-woven multifilament glass networks as related to composite processing", *Composites Manufacturing*, Vol. 4, no 4, 1993, pp. 199.
5. M. Spaid, F. Phelan, "Modeling void formation dynamics in fibrous porous media with the lattice Boltzmann method", *Composites Part A*, Vol. 29A, 1998, pp. 749.
6. C. Binétruy, B. Hilaire, J. Pabiot, "Tow impregnation model and void formation mechanism during RTM", *Journal of Composite Materials*, Vol. 32, no. 3, 1998, pp. 223.
7. L. Labat, J. Breard, S. Pillut-Lesavre, G. Bouquet, "Void formation prevision in LCM parts", *The European Physical Journal, Applied Physics*, Vol. 16, 2001, pp. 157.
8. N. Patel, L.J. Lee, "Modeling of void formation in liquid composite molding. Part II: Model development and impregnation", *Polymer Composites*, Vol. 17, no. 1, 1996, pp. 104.
9. N. Patel, L.J. Lee, "Modeling of void formation in liquid composite molding. Part I: Wettability analysis", *Polymer Composites*, Vol. 17, no. 1, 1996, pp. 96.
10. E. Ruiz, V. Achim, S. Soukane, F. Trochu, J. Bréard, "Optimization of injection flow rate to minimize micro/macro-voids formation in resin transfer molded composites", *Composites Science and Technology*, Vol. 66, 2006, pp. 475.
11. F. Trochu, R. Gauvin, D-M. Gao, "Numerical analysis of the resin transfer molding process by the finite element method", *Advanced Polymer Technology*, Vol. 12, no. 4, 1993, pp. 329.

Double scale porous media

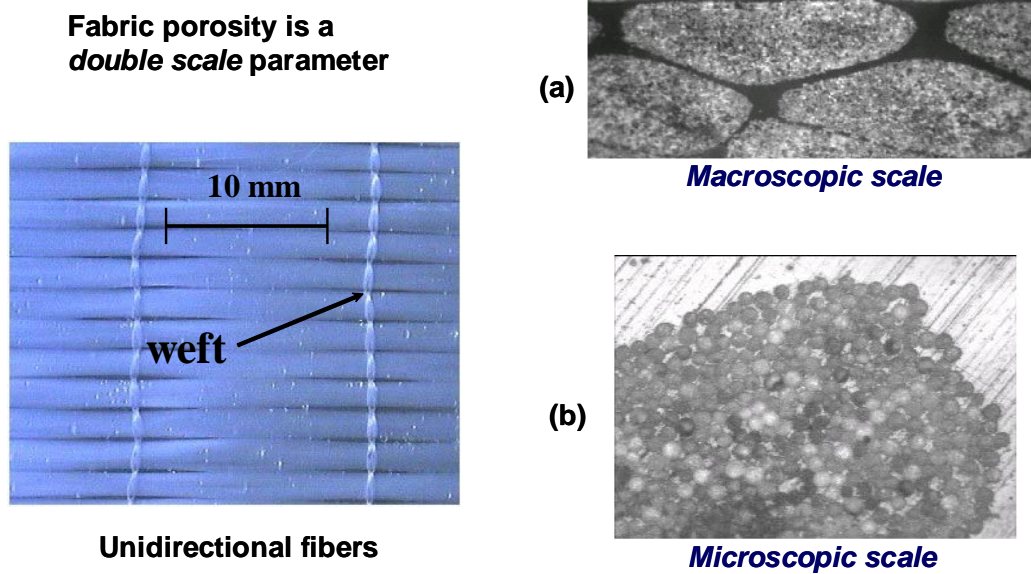


Figure 1. Fibrous reinforcements possess the structure of a dual scale porous medium: a) macroscopic voids can be observed between fiber tows; and b) microscopic voids exist between filaments.

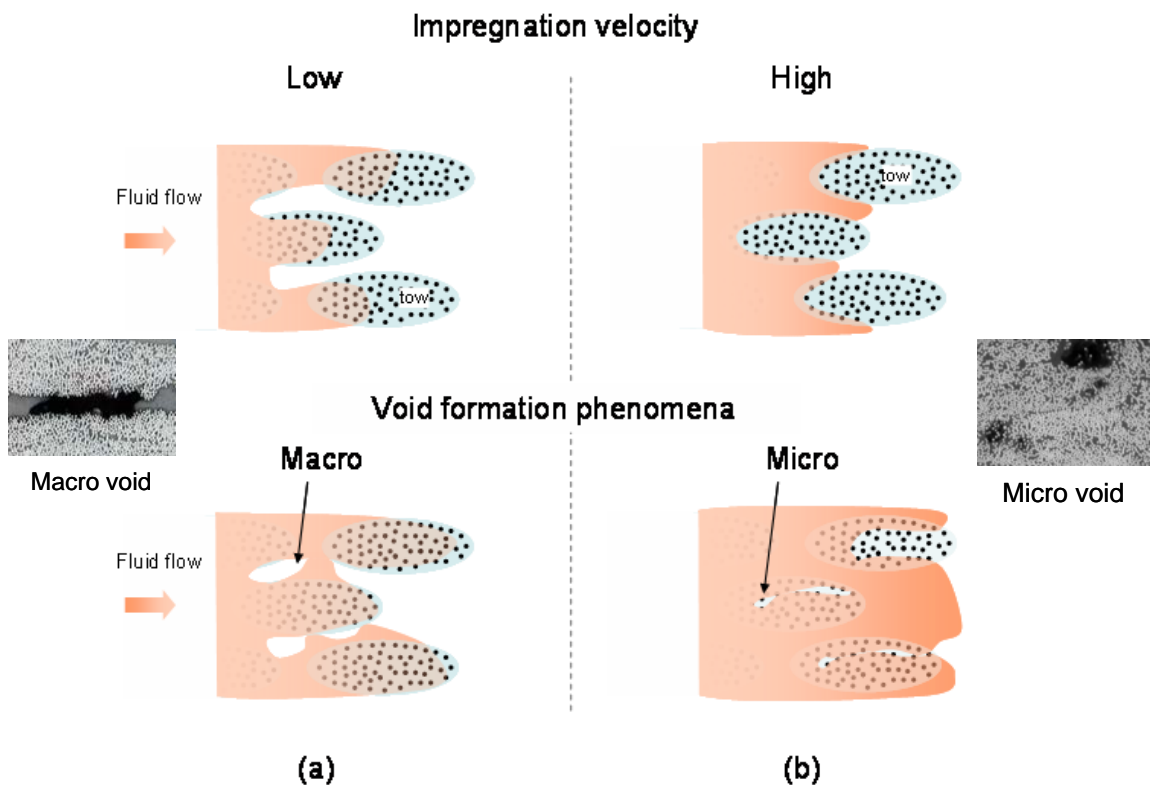


Figure 2. Impregnation mechanisms in a dual scale porous medium: (a) formation of macroscopic voids due to capillary forces (low resin velocity); and (b) formation of microscopic voids due to viscous forces (high resin velocity).

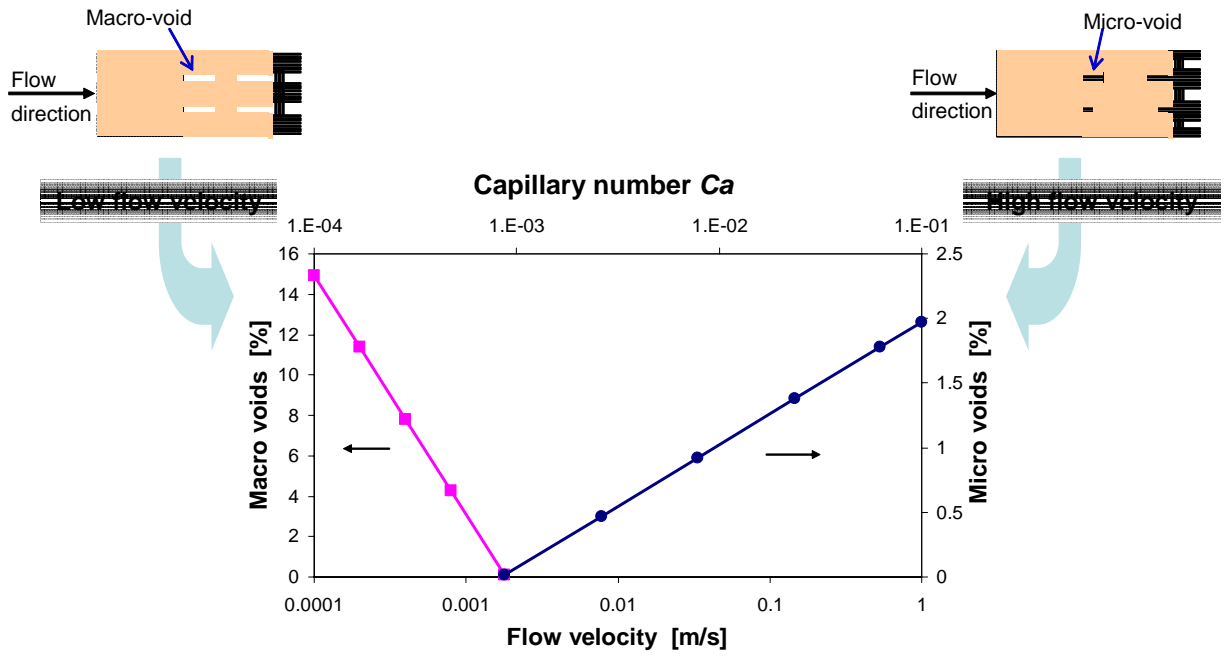


Figure 3. Macroscopic and microscopic void formation during fiber impregnation.

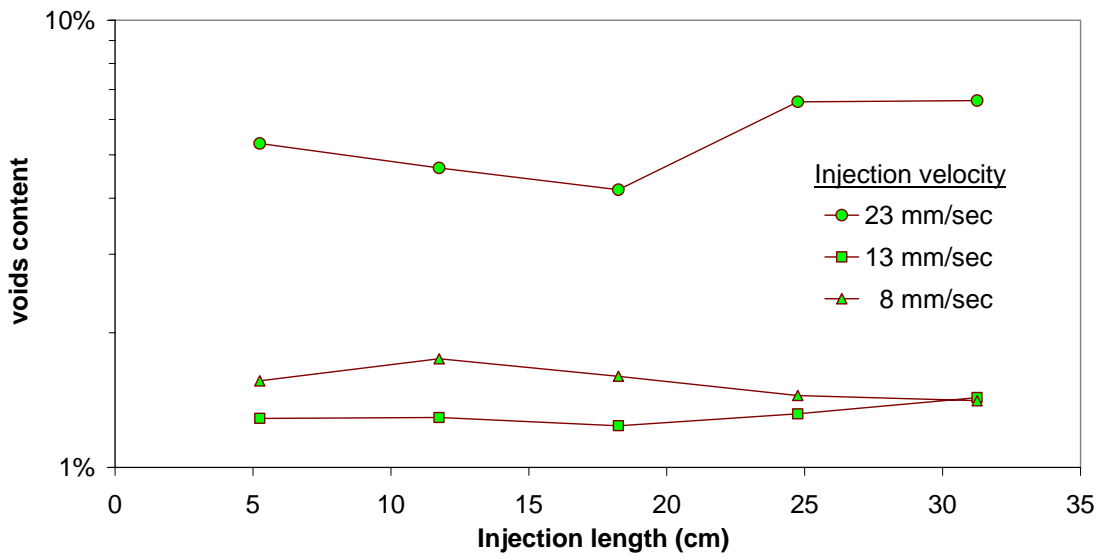


Figure 4. Measured void contents as a function of the injection length for the Unifilo 101 glass mat. Results for three injection flow rates are reported.

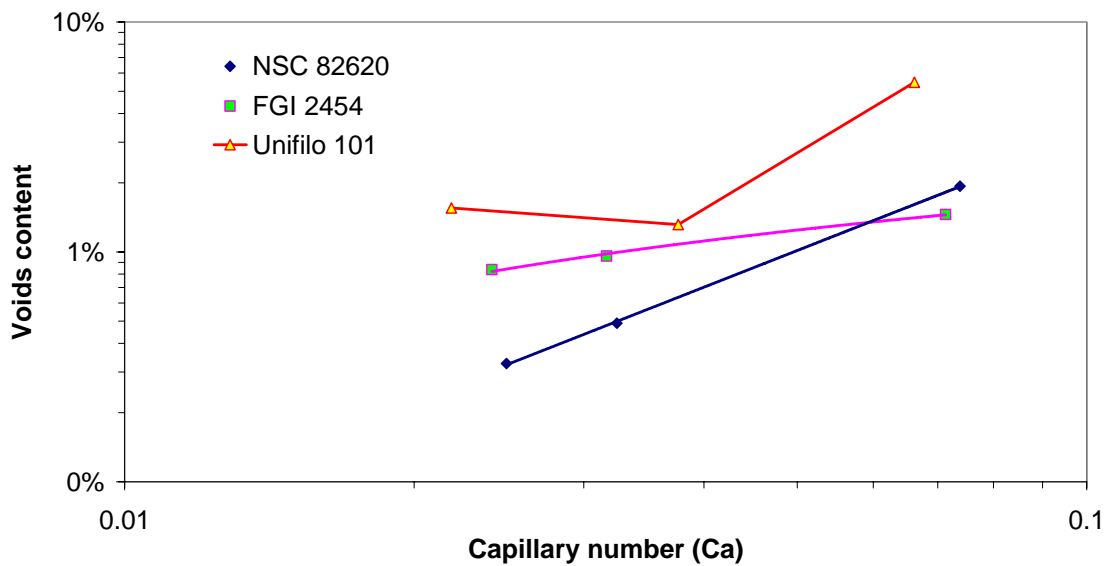


Figure 5. Measured void contents as a function of the capillary number for the 3 reinforcements tested. An optimal Ca exists for the Unifilo 101.

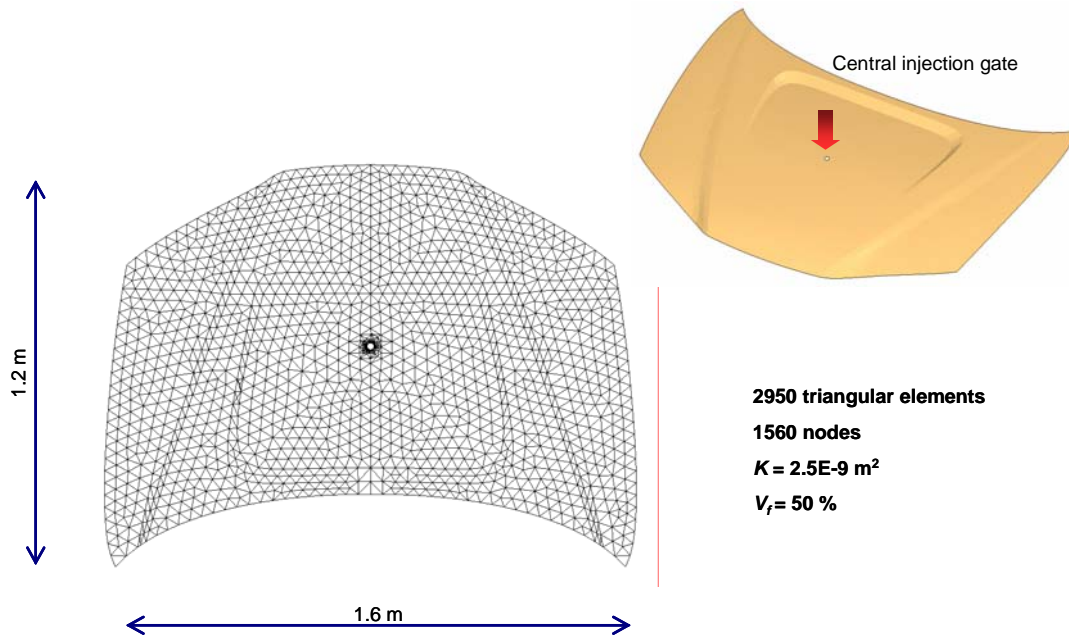


Figure 6. Geometry and 2D finite element mesh of the car hood used as application example.

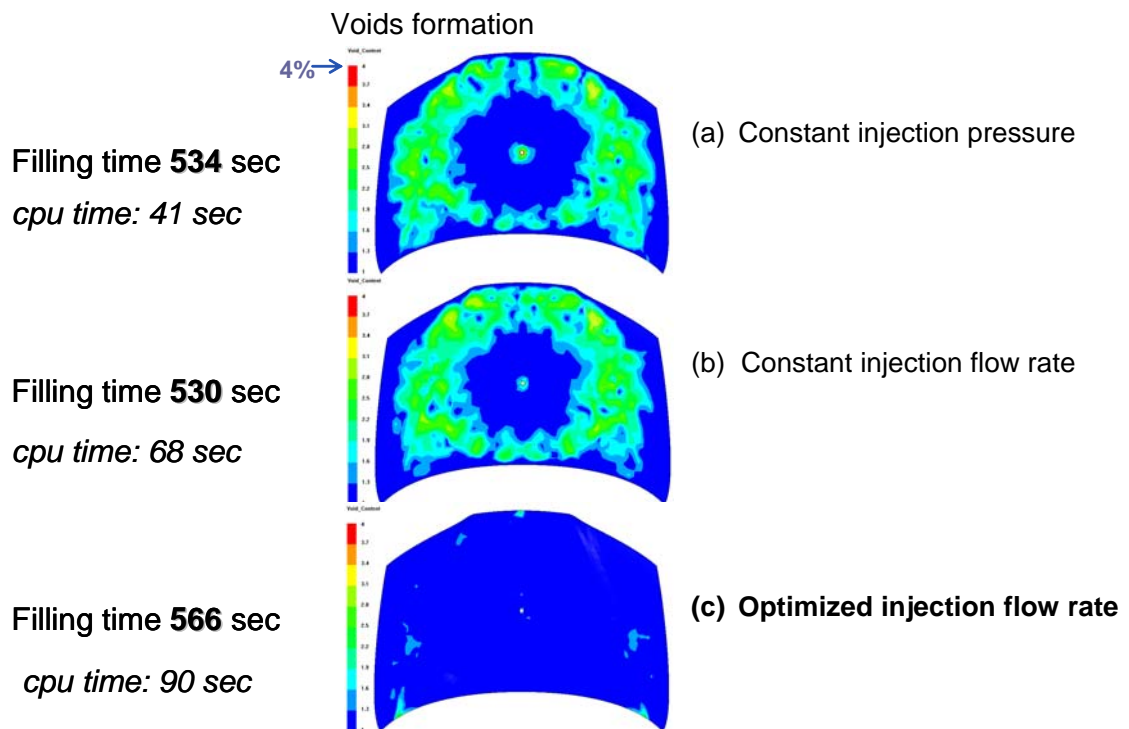


Figure 7. Comparison of calculated void formation on the car hood for three injection strategies.